INTERNATIONAL JOURNAL FOR NUMERICAL METHODS IN FLUIDS, VOL. 3, 591–604 (1983)

NUMERICALLY INDUCED OSCILLATIONS IN FINITE ELEMENT APPROXIMATIONS TO THE SHALLOW WATER EQUATIONS

ROY A. WALTERS

U.S. Geological Survey, M.S. 96, Menlo Park, CA 94025, U.S.A.

SUMMARY

Numerical noise has been a problem with finite element solutions to the shallow water equations. Two methods used to reduce the noise level are evaluated, and these results are compared with published results for equal-order interpolations. The two methods are mixed-interpolation (quadratic interpolation for velocity and linear interpolation for sea level) and a spectral form of the wave equation. Whereas mixed interpolation removes the troublesome sea level mode, it can still have considerable noise in velocity. The spectral wave equation is efficient and does not contain the spurious eigenmodes which contribute to high noise levels.

KEY WORDS Shallow Water Equations Finite Element Method Wave Equation Numerical Noise

INTRODUCTION

Numerical oscillations are a common occurrence in finite element simulations of various flow problems. Their existence is aptly demonstrated by Gray[1] and Gray and Lynch[2] for the shallow water equations and by Sani *et al.*[3] for the Navier–Stokes equations. The results of these two types of studies are bridged by a modal analysis,[4] where it is shown that the spurious modes in sea level in the shallow water equations behave similarly to the pressure modes in the Navier–Stokes equations. The existence of the sea level spurious modes is caused by anomalies associated with the application of the numerical solution method. The zero-frequency eigenmodes with a wavelength of twice the nodal spacing ($2d$) behave very differently from those in the continuum and are the source of the problem. In an important paper, Platzman[5] has introduced the concept of aliasing between long and short wave components due to a folded dispersion relation. This subject is examined in the discussion section.

Over the years three general methods have been employed to mitigate the effects of numerical oscillations: (1) damping the short wavelength modes, (2) generation of elements without spurious modes, and (3) modification of the governing equations.

Damping can include the use of spatial filters, the use of excessive viscosity or the use of dissipative time-stepping procedures. However, it is difficult to localize the effects of damping to small wavelengths only. The necessity for using damping is usually a consequence of a choice of an element that contains spurious modes. Furthermore, for most shallow water environments, one can show from scaling arguments that bottom friction dominates the effects of horizontal viscosity. Hence, viscous damping should only be used in a physically realistic sense, such as for a subgrid scale dissipation mechanism.

0271–2091/83/060591–14$01.40

Received 1 June 1982
Revised 7 October 1982

Dissipative time-stepping schemes are used relatively extensively with the shallow water equations. Gray and Lynch[2,6] have examined the ability of various time-stepping methods to numerically damp the modes of wavelength $2d$. However, as with the use of filters, the amount of damping is governed by grid spacing, timestep size, and other parameters, all of which are determined by network constraints and not by physical dissipation needs. Thus, the damping becomes a numerical artefact which is largely uncontrollable.

Some researchers have taken this method to the extreme and have formulated methods which severely attenuate waves with wavelengths of more than 50 times the grid spacing.[1]

In my own experiences, the use of damping in tidal models to remove small scale noise has not provided satisfactory results. As a result, I wish to concentrate on the latter two methods mentioned above. The desire to generate elements without spurious modes has led to the use of mixed interpolation. In this case a lower order interpolation is used for sea level, h, than that used for velocity, u, so as to cut off the wavelength for h at $4d$ and thereby eliminate the spurious oscillation mode. This method is used much more extensively in the solution of the Navier–Stokes equations[3] than in the shallow water equations. A typical 'good' element is the 6-node triangle with quadratic velocity and linear h. Unfortunately, simpler triangular and quadrilateral elements with linear velocity and constant surface elevation (over an element) have numerical problems—the 3-node triangular element will not converge when large numbers of elements are used[7] and the 4-node quadrilateral element has a single spurious mode. Of the commonly used linear and quadratic elements, the 6-node triangle and the 9-node quadrilateral with mixed interpolation have both an absence of spurious modes and favourable convergence properties.[4] That is not to say that other usable elements do not exist; rather, they have yet to be identified and/or tested. The eigenmode analysis provides a simple means of determining valid elements.

Finally, one can convert the governing equations into a set of equations which have the property that all wavelengths propagate and there are no zero frequency spurious mode solutions. The most common method is to convert the continuity equation into the form of a wave equation. This method is, in fact, used more extensively than the literature would suggest. As an example, it is used in conjunction with tidal harmonics by Pearson and Winter[8] and in conjunction with explicit and implicit time-stepping procedures by Lynch and Gray.[9] For simulations where the surface elevation but not discharge is desired, this method may be particularly useful because of the economy in solving for only one dependent variable (for the linearized equations) on a relatively coarse mesh.

In earlier papers, Gray and Lynch[2] and Lynch and Gray[9] compare the accuracy of a primitive equation formulation of the shallow water equations with two modified forms, a semi-implicit method and a wave equation method. Whereas the modified forms generally performed well, the primitive equation form contained spurious oscillation modes in sea level and thus performed poorly. In the study presented here, the results for the primitive equations using mixed interpolation are added to this comparison and remove the effects of the sea level modes (option 2, above). In addition, results are presented for a spectral form of the wave equation (option 3, above). When the energy spectra of sea level and velocity can be represented by line spectra, it is highly efficient to compute the Fourier amplitudes directly. Furthermore, the solution method has all the advantages of the wave equation schemes.

In the following sections the governing equations are defined followed by a description of the numerical experiments and the numerical results for the various interpolation methods. These results are compared with the results using a wave equation formulation. The physical implications and limitations of these methods are discussed.

GOVERNING EQUATIONS

The governing equations used in this analysis are the shallow water equations which are derived by vertically integrating the Navier–Stokes equations for a fluid flow with a free surface.[10] These equations are applicable to gravity-wave propagation in a fluid of constant density where the wavelength is much greater than the depth. They are

the x-equation of motion,

$$\frac{\partial u}{\partial t}+u\frac{\partial u}{\partial x}+v\frac{\partial u}{\partial y}-fv+g\frac{\partial h}{\partial x}-\frac{1}{(H+h)}\left\{\frac{\partial}{\partial x}[(H+h)\tau_{xx}]+\frac{\partial}{\partial y}[(H+h)\tau_{xy}]+\tau_x^s-\tau_x^b\right\}=0 \quad (1)$$

the y-equation of motion,

$$\frac{\partial v}{\partial t}+u\frac{\partial v}{\partial x}+v\frac{\partial v}{\partial y}+fu+g\frac{\partial h}{\partial y}-\frac{1}{(H+h)}\left\{\frac{\partial}{\partial x}[(H+h)\tau_{yx}]+\frac{\partial}{\partial y}[(H+h)\tau_{yy}]+\tau_y^s-\tau_y^b\right\}=0 \quad (2)$$

and the continuity equation,

$$\frac{\partial h}{\partial t}+\frac{\partial}{\partial x}[(H+h)u]+\frac{\partial}{\partial y}[(H+h)v]=0 \quad (3)$$

where density is assumed constant; x, y are Cartesian co-ordinates in the horizontal plane (m); u, v are depth-averaged velocity components in the x, y directions (m/s); t is time (s); h is water-surface elevation measured from mean water depth (m); H is mean depth of the water column (m); $f=2\Omega\sin\theta$ is the Coriolis parameter (s^{-1}); Ω is rotation rate of the earth (s^{-1}); θ is latitude (deg); g is gravitational acceleration (m/s^2); τ_{xx}, τ_{xy}, τ_{yx}, and τ_{yy} are a combination of molecular and Reynolds stresses, and dispersion terms (m^2/s^2); τ_x^s and τ_y^s are components of the surface wind stress (m^2/s^2); and τ_x^b and τ_y^b are components of the bottom stress. The Reynolds stress terms are approximated by a symmetric stress tensor with an eddy viscosity coefficient adjusted empirically. (Viscosity is not used in the wave equation formulations.) Because these stresses are generally small compared with bottom friction for the shallow estuarine environments considered here, the eddy viscosity coefficient is kept at a small value (1–1000 cm^2/s depending upon refinement) only to dissipate the energy cascaded to shorter wavelengths owing to the non-linear nature of the model (see discussion section). The surface stresses are specified by a quadratic form of the wind velocity. The Manning–Chezy formulation for bottom stress in open channel flows is extended to two dimensions to give the bottom stress. For further details see Reference 11.

The boundary stresses at the surface and bottom are explicitly included in the governing equations. As can be shown by scaling, the lateral stresses are important only in the lateral boundary layer along the shoreline (or perhaps in internal shear layers) for the shallow estuarine environments considered here. Because the computational grid in a numerical model is typically larger than the thickness of the shoreline boundary layer, setting the tangential velocity to zero along the boundary can distort the velocity field to an unrealistic extent. For this reason, no-slip conditions are relaxed at the shoreline and parallel flow and zero stress conditions are applied such that there is no mass flux across the boundary. Note, however, that when steep shorelines are present, the lateral boundary layer must be taken into account.[12]

At open boundaries, the water surface elevation and (or) the current velocity can be specified so long as the system is not overconstrained. Along these boundaries, the tangential shear stress also vanishes. When the Coriolis force is included, there is some difficulty in the

open boundary condition owing to the lateral head gradient. Using a constant surface elevation causes the velocity to enter and exit at large angles with the normal to the boundary as well as creating a 'half eddy' circulation pattern.[12] This problem is largely nullified by using a direction–elevation condition where elevation is specified at a central node and the velocity direction is specified at all the nodes on the open boundary.[11,12]

Primitive formulation

The finite element method is applied to (1)–(3) by discretizing the spatial domain into elements which are usually of triangular or quadrilateral shape. Depending on the element type, the discretized values for velocity and depth are located at nodes which may be at the vertices, along the sides, or in the interior of the elements. The value of a variable within an element is found by interpolating from the values at the element nodes with the use of basis or interpolation functions. (See Reference 13 for further details.) The elements used in this analysis are the 6-node triangle and the 3-node triangle, although results from Reference 2 for 9-node quadrilaterals are also noted.

The velocity and surface elevation within an element are interpolated as $\mathbf{u} = [\mathbf{N}]\{\mathbf{u}\}$ and $h = [\mathbf{M}]\{\mathbf{h}\}$ where $[\mathbf{N}]$ are the basis functions for velocity, $[\mathbf{M}]$ are the basis functions for sea level, and $\{\mathbf{u}\}$ and $\{\mathbf{h}\}$ are the column vectors of the nodal values of velocity and sea level, respectively. The residual for the shallow water equations can be evaluated by substituting in the interpolated values for the respective variables. The weighted residual is found by multiplying each equation by each of the corresponding nodal interpolation functions and integrating over the element. The resulting weighted residuals are set equal to zero. The element contributions are then summed into a global matrix, which may be efficiently solved by a frontal solver[14] or by other sparse solution techniques. In the weighted residual, the stress terms are expanded and expressed in a divergence form; the order of these terms is reduced by the use of integration by parts. Further, the dispersive stress terms containing gradients in depth are neglected.[11] As a result, the governing equations can be written in matrix form as,

$$\begin{aligned}
&\mathbf{M}\frac{\mathrm{d}\mathbf{u}}{\mathrm{d}t} + \mathbf{A}\mathbf{u} - f\mathbf{v} + g\mathbf{C}_x\mathbf{h} + \mathbf{T}_x = \mathbf{F} \\
&\mathbf{M}\frac{\mathrm{d}\mathbf{y}}{\mathrm{d}t} + \mathbf{A}\mathbf{v} + f\mathbf{u} + g\mathbf{C}_y\mathbf{h} + \mathbf{T}_y = \mathbf{G} \\
&\mathbf{M}'\frac{\mathrm{d}\mathbf{h}}{\mathrm{d}t} + \mathbf{R}(\mathbf{u}, \mathbf{h}) = \mathbf{0}
\end{aligned} \tag{4}$$

where $\mathbf{u}, \mathbf{v}$ and $\mathbf{h}$ are the nodal values for velocity and sea level. The detailed form of the matrices follows from (1)–(3) and is given in Reference 11. The equations are integrated in time using a time-centred scheme[11] and a semi-implicit scheme.[15]

Spectral wave equation formulation

The wave equation form of the governing equations is derived by Lynch and Gray[9] by differentiating the continuity equation (3) with respect to time and substituting (1) and (2) for u and v, respectively. The resulting equations can be integrated in time using either explicit or implicit methods.[9] In addition, a comparison between the time-stepping and continuous in time (spectral) approaches is presented by Lynch.[16] He finds that these approaches are equivalent for $\Delta t \rightarrow 0$ in the former method.

The form of the governing equations used here is similar to that presented by Pearson and Winter[8] and extended by Jamart and Winter.[12] (Also see References 16 and 17). Each of the dependent variables is considered to vary periodically with frequencies ω_n, which are specified beforehand:

$$\begin{Bmatrix} u_n \\ v_n \\ h_n \end{Bmatrix} = \begin{Bmatrix} u_{0n} \\ v_{0n} \\ h_{0n} \end{Bmatrix} \exp(-i\omega_n t) \tag{5}$$

where u_n is the velocity associated with the nth frequency, h_n is the corresponding sea level, u_{0n} and h_{0n} are the corresponding modal amplitudes, and ω_n is the angular frequency of the nth mode. The instantaneous values for the dependent variables can be found by synthesis:

$$\begin{aligned} u &= u_0 + \sum_{n=1}^{N} u_{0n} \exp(-i\omega_n t) \\ v &= v_0 + \sum_{n=1}^{N} v_{0n} \exp(-i\omega_n t) \\ h &= h_0 + \sum_{n=1}^{N} h_{0n} \exp(-i\omega_n t) \end{aligned} \tag{6}$$

These approximations for u and h are then substituted into the equations of motion (1)–(3). Multiplying each equation by $\exp(i\omega_n t)$ and integrating over time, one derives the modal equations for the amplitudes.[8] Finally, the modal amplitudes for velocity are eliminated from the continuity equation with the use of the momentum equations. In the linearized form, the resulting equation is as follows:

$$i\omega h + \nabla \cdot \left\{ gH \left[\frac{q^2}{q^2+f^2} \right] \nabla h \right\} + f \left\{ \frac{\partial}{\partial x} \left[\left(\frac{gH}{q^2+f^2} \right) \frac{\partial h}{\partial y} \right] - \frac{\partial}{\partial y} \left[\left(\frac{gH}{q^2+f^2} \right) \frac{\partial h}{\partial x} \right] \right\} = 0 \tag{7}$$

where the advective terms (which contribute to the higher harmonics) and the surface wind stress are neglected, $q = -i\omega_n + \tau$, and τ is the linear coefficient for bottom stress. The full formulation of (7) may be found in Reference 8. The velocity can be calculated either from numerical differentiation[8,12] or by a FE approximation to the momentum equations. The latter method is used here and the resulting matrix equations are derived from (2) and (3) as before in (4). The equations are assembled and solved in the same manner as with the primitive equations. However, the equations are solved sequentially here rather than simultaneously. First the wave equation is solved for the complex modal amplitudes for sea level using the initial approximation for velocity. Then the momentum equations are solved using the new sea level modal amplitudes. For the non-linear system with advective terms and quadratic bottom stress, this solution is iterated until a convergence criterion is satisfied.

Because I wish to compare the numerical results with analytical solutions, I use linearized bottom stress. Hence the equations for the fundamental frequencies are linear; the non-linear advective terms appear as forcing functions for the higher harmonics. As the dimensions in the numerical experiments make the non-linear terms negligible, I only calculate the amplitudes of the fundamental.

NUMERICAL EXPERIMENTS

Almost any numerical scheme will give reasonable results for a periodic forcing of a rectangular basin of constant depth.[1] As demonstrated by Gray and Lynch,[2] both depth

variations and lateral variations in geometry can be used to test the sensitivity of various solution methods to the occurrence of short wavelength oscillations. What appears to matter is not how the variations are introduced but rather the resultant velocity and sea level gradients, particularly near the solid end boundary (in essence, the short wavelength modes are forced by a Gibbs' phenomenon at the boundary). Large magnitude, small-scale variations cause steep gradients and strong oscillations in those models which are susceptible. The 6-node triangular network chosen for testing is the rectangular basin in Figure 1. For constant and linearly varying depth, good results are derived using equal order interpolation and mixed interpolation,[2,11] and using the wave equation formulation.[9] For quadratically varying depth, Gray and Lynch[2] show that equal order interpolation leads to serve internode oscillations whereas the wave equation approach with time-stepping does not. Equivalent results were obtained with a quarter annulus network.[2] The quadratically varying depth for a rectangular basin is used in this study to test the sensitivity of mixed interpolation methods and a spectral form of the wave equation.

The test network has the same size and boundary conditions as that described by Gray and Lynch (Reference 2, Figure 1c) and shown here in Figure 1 for 6-node triangles. The network with 3-node triangles is generated by subdividing each of these 6-node triangles into four 3-node triangles. The basin has solid boundaries on three sides and a periodic variation in sea level imposed at the open boundary. Along the top and bottom boundaries, the normal component (v) of velocity is set to zero, whereas on the left solid boundary both components of velocity are set to zero. The variation in sea level on the right is specified as $a \cos(\omega t)$ where $a = 0{\cdot}03048$ m ($0{\cdot}1$ ft) and $\omega = 2\pi/T$ where $T = 12{\cdot}4$ h. The network is six nodal spacings across and eight nodal spacings high ($6d$ by $8d$, where $d = 15{\cdot}240$ m (50,000 ft)). The bottom friction was linearized as $\tau_0 = \tau u$, where $\tau = 10^{-4}$ and the Coriolis parameter was set to zero ($f = 0$).

For the time-stepping methods, the simulation was started at rest at $t = 0$ and continued until a periodic solution was obtained (usually during the third or fourth cycle). Fifty timesteps per cycle were used. Although the non-linear advective terms were retained in the

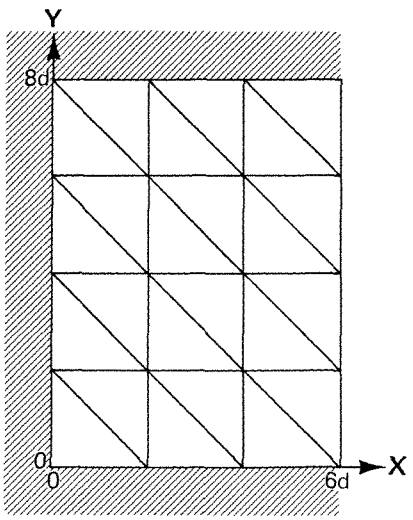

Figure 1. The numerical grid used for the numerical tests (identical to the grid in Figure 1(c) of Reference 2). The sea level is specified as a periodic function on the right with amplitude of 0·03048 m and period of 12·4 h. The nodal spacing is 15,240 m. The depth varies quadratically as $h = 3{\cdot}048[(3/2)(x/L)+1]^2$ where $x = 0$ on the left boundary

time-stepping models, their effects were negligible owing to the small amplitude wave. This fact has been verified by subsequent simulations. In keeping with this approach, only the amplitudes of the fundamental frequency are calculated in the spectral model.

Using 9-node quadrilaterals, the solution for the primitive equations was derived by Gray and Lynch[6] and is shown in Figures 2 and 4 (EOI9) for the in-phase (cosine) component of h and u. As may be noted, there are severe oscillations in h and u. Considerably better results were derived here using 6-node triangles (EOI6). I feel that the larger oscillations in the quadilaterals are due to the lower accuracy caused by the low order numerical integration (9-point Simpson's rule using the nodes for the quadrilaterals vs. 7-point Gauss rule for the 6-node triangles).

The results for a 6-node triangular network with quadratic velocity and linear surface elevation are shown in Figures 2 and 3 for the in-phase and quadrature (sine) component of h, and in Figures 4 and 5 for the in-phase and quadrature component of u. Because the two time-stepping methods gave the same results, only the time-centred results are given here (MI). Although the sea level oscillation mode is removed, there is an oscillation in u due to the small-scale forcing in depth near the solid boundary, and this oscillation has larger magnitude than the case with equal order interpolation with the same elements (6-node triangles). As the velocity gradient is increased owing to a reduction in depth, the oscillation becomes larger. Horizontal eddy viscosity is used in this model with values of 1000 cm^2/s, which is at the upper limit for this size of grid spacing. As a note, viscosity values of 10^6 to 10^7 cm^2/s are required to damp these oscillations, whereas the solution will not converge with zero viscosity. The larger values are orders of magnitude larger than those one would expect to find in nature for these length scales.

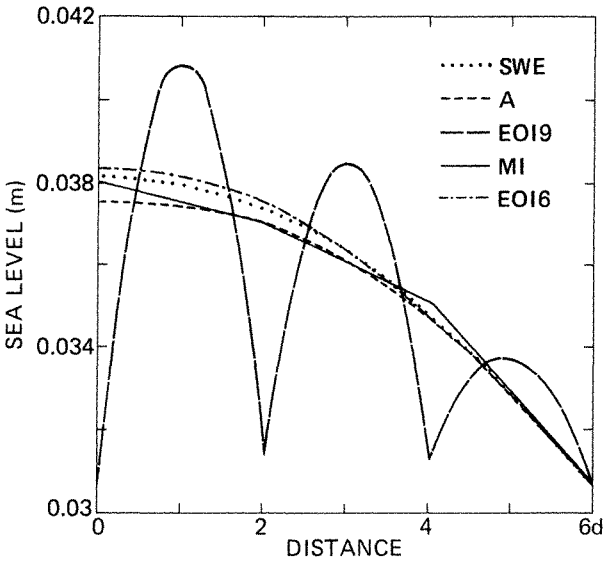

Figure 2. Sea level variations in the x-direction when the sea level at the boundary is at a maximum ($\omega t = 0$). A, analytical solutions; EOI9, quadrilateral elements with quadratic, equal-order interpolation (9 node); EOI6, triangular elements with quadratic, equal-order interpolation (6 node); MI, triangular elements with quadratic-linear, mixed interpolation (6 node); SWE, harmonic solution using 6-node triangles with equal-order interpolation. The solution for the quadrilateral is from Reference 2, and the analytical solution is described by Lynch and Gray[9]

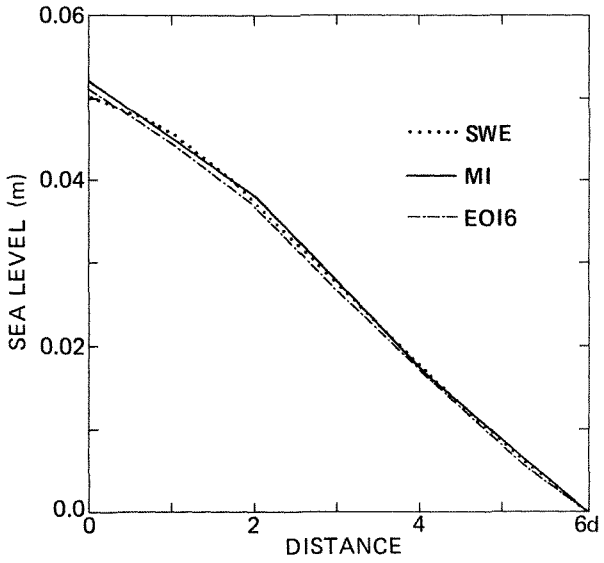

Figure 3. Sea-level variations in the x-direction when the sea level at the boundary is zero ($\omega t = \pi/2$). The symbols are the same as Figure 2

Finally, the results using the spectral wave equation are also shown in Figures 2–5 (SWE). Both the sea level and velocity exhibit smooth variations across the network and agree with the analytical solution. Using the 6-node triangular elements, this method was about 50 times more efficient in computer time than using the mixed interpolation form of primitive equations with a semi-implicit time-stepping procedure and about 250 times more efficient than the time-centred scheme with Newton–Raphson iteration.

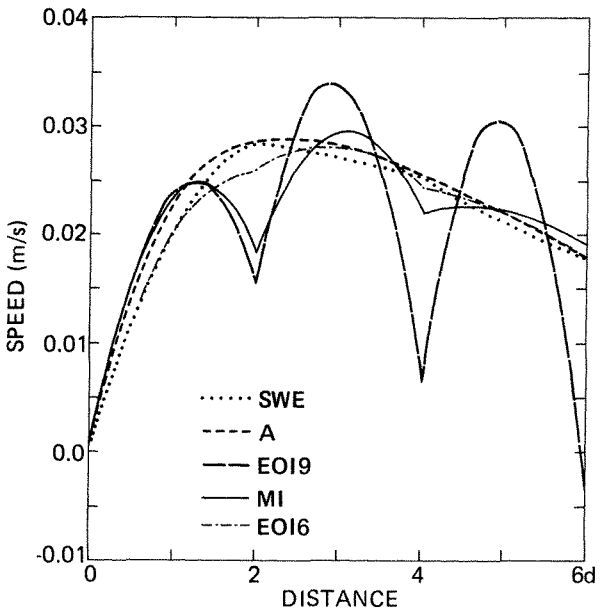

Figure 4. Velocity component in the x-direction computed when the sea level at the right boundary is at a maximum ($\omega t = 0$). The symbols are the same as Figure 2

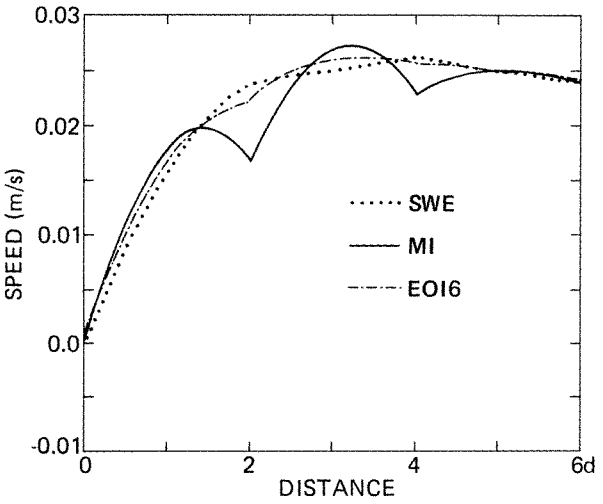

Figure 5. Velocity component in the x-direction computed when the sea level at the right boundary is zero ($\omega t = \pi/2$). The symbols are the same as in Figure 2

DISCUSSION

In order to interpret the numerical results, I wish to present an overview of the applicable theoretical analysis. First I will consider the more straightforward case of the zero frequency modes and then the more general case of time dependent modes.

The sensitivity of various numerical schemes to numerical oscillations is generally determined by the wave behaviour at small wavelengths, specifically at the wavelength $2d$ defined by the grid spacing. An eigenmode analysis of various finite element discretizations of the shallow water equations has been presented by Walters and Carey.[4] The general method is similar to a Fourier analysis of the discretized governing equations, (1)–(3). First the dependent variables are decomposed into a set of periodic disturbances of the form

$$(u, v, h) = (u_0, v_0, h_0) \exp \mathrm{i}(kx + my - \omega t) \tag{8}$$

where ω is angular frequency and k, m are wavevectors in the x, y directions, respectively. Using this relationship in (1)–(3) where only the gravity wave terms are included, one derives the dispersion relation for a continuum:

$$\omega^2 = c^2(k^2 + m^2) \tag{9}$$

where $c^2 = gH$ is the shallow water phase speed.

The corresponding dispersion relations for representative numerical schemes for approximating the shallow water equations can be found by discretizing (1)–(3) in space, then applying (8). Following this, the eigensolutions for simple grids are found and these solutions are examined with respect to the occurrence of spurious modes.

Consider as an example, the one-dimensional element with linear interpolation for both h and u (LL). The dispersion relation for this scheme is given by

$$\omega^2 = \frac{gH}{d^2}\left(\frac{3 \sin (kd)}{2 + \cos (kd)}\right)^2 \tag{10}$$

and is shown in Figure 6, where both the frequency and wavevector have been normalized as

$$\Omega = \frac{\omega d}{\pi c}, \qquad K = \frac{kd}{\pi} \tag{11}$$

so that for the exact solution $\Omega = K = 1$ for a wave with the minimum allowable wavelength in the grid ($2d$). For the numerical approximation (LL, Figure 6), Ω never attains unity but returns to zero at a wavelength of $2d$. Because the curve is not monotonic, for a given value of ω we may have multiple values of k. In particular, the occurrence of an eigenmode with $\omega = 0$ and a finite k is an anomaly that is associated with the spurious mode. For an enclosed domain with n elements each of length L with the boundary conditions $u = 0$ at $x = 0$ and L, the eigensolutions are for $j = 0, 1, 2, \ldots, n$

$$\begin{aligned} h_j &= \cos(kx_j)\cos(\omega t) \\ u_j &= (g/H)^{1/2}\sin(kx_j)\sin(\omega t) \\ k &= (1, 2, 3, \ldots, n-1)/L \end{aligned} \tag{12}$$

where h_j and u_j are the nodal values for sea level and for velocity. There are two solutions where $\omega = 0$. One is the hydrostatic solution where $k = 0$ with $h_j = 1$. The other is the spurious mode where $k = \pi/d$ and $h_j = (-1)^j$ and $u_j = 0$. The presence of this mode is a numerical artefact which is introduced by the finite spatial discretization of the shallow-water equations and it corresponds to internode oscillations in sea level of wavelength $2d$. As an alternative interpretation, one can consider this mode as corresponding to a physical eigenmode of the continuous problem which has its phase speed reduced to zero by the numerical method and appears as a stationary internode oscillation. A similar analysis holds in two dimensions. Again, because $\omega = 0$ and $u_j = 0$ for this mode, the governing equations

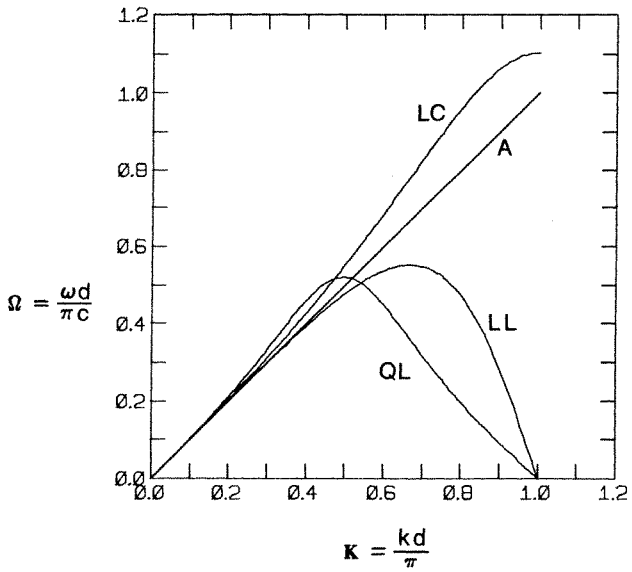

Figure 6. One-dimensional dispersion relation for various schemes: A, continuum; LL, element with linear velocity and linear sea level; LC, element with linear velocity and piecewise constant sea level; QL, element with quadratic velocity (three nodes) and linear sea level (two end nodes)

(1) to (3) reduce to

$$u = 0, \qquad v = 0, \qquad \nabla h = 0 \tag{13}$$

Of special significance is the fact that the spurious mode is stationary. It is forced by small scale irregularities in forcing data and in the network. When the force vector has a projection in this node (such as a singularity or the occurrence of boundary layers) the spurious mode will be forced. Because this mode satisfies the homogeneous equation for $\omega = 0$, an arbitrary multiple of this mode can be added to the solution with no effect upon the dynamics, a feature which can raise serious questions about proper convergence.

The one-dimensional dispersion relation for the mixed-interpolation scheme (QL) is also shown in Figure 6 where d is the spacing between the velocity nodes. Because sea level is interpolated linearly, its minimum wavelength is $4d$ rather than $2d$ for the velocity. Hence, there is no zero frequency spurious sea-level mode in this case. The extension to two dimensions is straightforward[4] with the result that the 6-node triangle and the 9-node quadrilateral with quadratic velocity and C^0 linear sea level contain no spurious sea level modes.

A particularly interesting case is that of the quadrilateral element with bilinear velocity and piecewise constant sea level (LC). The one-dimensional relation for LC is shown in Figure 6. In this case, there is no zero frequency spurious mode. By staggering the velocity and the sea level nodes, one creates an artificial grid spacing of $d/2$, where d is the distance between adjacent nodes for the same solution field variable. Thus, the $\omega = 0$ solution is moved down in wavelength to d which is below the cutoff wavelength for the grid.

However, the two-dimensional case is not so well behaved. For a wave which propagates diagonally to the grid directions ($k = m$), there is again an $\omega = 0$ eigenmode for $k = m = \pi/d$. This mode is in fact the infamous 'chequerboard' mode which satisfies

$$\mathbf{u} = 0, \qquad \nabla h = 0 \tag{14}$$

and describes a piecewise-constant oscillation in sea level on alternate elements or grid blocks.

Finally, one can modify the shallow water equations to form a wave equation to replace the continuity equation. This method is analysed in detail by Lynch and Gray[9] and is characterized by monotonically increasing curve for ω vs. k. As a result, the spurious, zero frequency solution does not exist in this case. Furthermore, a subgrid-scale dissipation model is apparently unnecessary because the short wavelength modes readily propagate through the network and thus do not accumulate energy. This last point underlines a fundamental difference between wave equation and primitive equation models.

The dispersion analysis and modal behaviour described above concern the $\omega = 0$ modes or steady-state modes. These will result if an initial value problem evolves to a steady state. The behaviour of the time-dependent modes is analysed in a significant paper by Platzman[5] who introduces the important concept of aliasing between wavevectors. Introducing this idea into the present analysis, we note that the solution corresponding to $\omega = 0$ and $k = 0$ has as its alias the (spurious) mode $\omega = 0$, $k = \pi/d$. Further, the basic problem with extraneous modes is due to the fact that there are multiple roots for k as a function of ω (LL, QL in Figure 6). In the numerical problem here, a rectangular embayment is forced with a sea level that varies periodically with an angular frequency ω. For those schemes which have folded dispersion relations, both a long wave (desired) and a short wave (noise) component will be forced. The relative amplitude of these two components depends upon their respective admittances and is discussed in detail by Platzman.[5] A serious problem occurs when the

wavelength of the spurious mode corresponds to a resonance of the basin, in which case the short wavelength mode can be relatively large.

For the basin used in the numerical experiments, the spurious mode is far removed from a resonance, hence any of the numerical schemes can give good results for the constant depth case. However, for the quadratically varying depth, the short wavelength modes are forced directly by small scale variations in depth. From an examination of the results, the observed modes are not the zero frequency modes but rather the time-dependent (aliased) modes. Hence there is a coupling between u and h via the time rate of change terms in (1) to (3) which is absent in the zero frequency modes. The modes in the results appear to be generated by the sharp gradient in velocity at $x = L$, the closed boundary. The resultant oscillations in velocity are akin to a Gibbs' phenomenon from the coarse nodal spacing and are coupled into sea level for LL or any other scheme which allows the short wavelength mode in sea level.

The results for equal-order interpolation using both linear and quadratic elements were very sensitive to the network layout. For the network in Figure 1, there is an asymmetry from top to bottom, whereas the nodal support is homogeneous in the interior. Thus there tends to be a slope in the solution such that high values in sea level occur on one side and low values on the other. The solutions nearest these sides exhibit the most noise. The greatest amount of noise was generated using an inhomogeneous network where the nodal support varies from 4 to 8 elements at the corner nodes. The resulting errors have a strong projection in the spurious mode as one may see in the analysis of Platzman.[5]

Although mixed interpolation removes the spurious mode in sea level, it is still subject to the short wavelength mode in velocity. There is more energy being accumulated than can be dissipated with realistic values of eddy viscosity. This can be demonstrated numerically with the use of constant depth, linearly varying depth, and quadratically varying depth in the rectangular network. In the first, viscosity is not required; in the second, moderate values are required, whereas in the last large values are required. Refinement can be of help in that it removes the short wavelength forcing (effectively, it moves it to longer wavelengths) and thus does not excite the troublesome eigenmodes. However, the problem here is clearly not the fault of an improper subgrid-scale model; rather, it is due to the poor phase speed accuracy at small wavelengths.

There are, in fact, other problems with these mixed-interpolation elements that are related to the fact that they are underconstrained with respect to continuity. In the continuum, the ratio of continuity equations to momentum equations is 1/2 (in two dimensions). However, for the 6-node triangle the constraint ratio is about 1/6, depending upon the element support of the corner nodes. When Dirichlet conditions on sea level are specified, the additional loss of continuity equations leads to poor velocity accuracy.[11] Although the spurious sea level mode does not appear with mixed interpolation as used here, the level of noise in the velocity solution is generally somewhat larger than equal order interpolation (quadratic u and quadratic h). This appears to be due to the low constraint ratio and is common to all the simulations performed in the course of this analysis.

The wave equation models maintain relatively good phase speed for all wavelength disturbances within the network. As may be seen, both the time-stepping[9] and spectral forms of the wave equation gave good results for this difficult network (in the sense that large depth variations forced small wavelength modes). Thus one may surmise that propagation of the short wavelength eigenmodes (a monotonically increasing dispersion relation) rather than viscous damping is the more effective means of removing these modes from the network.

Further, the spectral form of the wave equation is a very efficient method of solving

problems with periodic forcing, i.e. those characterized by line spectra. For aperiodic forcing during a finite time interval, time-stepping methods are easiest to use, although one may still approximate a continuous spectrum and solve for the Fourier coefficients.

In spite of the good results, the wave equation approach is not without some difficulties. First, the coding is more complicated owing to the added complexity of the wave equation over the continuity equation, although this problem is not serious. Second, the wave equation approach has not been used extensively enough to define what forms of the momentum equations are most advantageous to use.[9] For instance, Pearson and Winter[8] interpolate velocity directly from the solution for h. On the other hand, the method presented here solves the finite element approximation to the momentum equations after solving the wave equation for h. The latter method is about a factor of 2 less efficient in run time but probably results in a better global approximation of the velocity field.

CONCLUSIONS

1. Using elements with equal-order interpolation and the primitive form of shallow water equations, short wavelength oscillations are present in most solutions except for trivial networks.
2. Mixed-interpolation elements show improved results for sea level; however, the velocity is still subject to short wavelength oscillations owing to poor phase speed behaviour and is generally inferior to the velocity solution using equal-order interpolation. For the more difficult networks with small-scale forcing, these oscillations cannot be removed with reasonable amounts of eddy viscosity which is used in an approximation to subgrid-scale dissipation.
3. Wave-equation formulations are in general insensitive to short wavelength oscillations, primarily due to the good phase speed response. Depending upon the specific application, either time-stepping[9] or spectral methods may be used. The latter is more ideally suited to problems with a small number of well-defined frequencies, such as tidal oscillations.

ACKNOWLEDGEMENTS

I wish to acknowledge Drs. G. F. Carey, W. G. Gray and D. R. Lynch for their helpful comments and discussions.

REFERENCES

1. W. G. Gray, 'Do finite element models simulate surface flow?' *Proceedings of the Third International Conference on Finite Elements in Water Resources*, International Society for Computational Methods in Engineering, University of Mississippi, Oxford, May 1980.
2. W. C. Gray and D. R. Lynch, 'On the control of noise in finite element tidal computations: a semi-implicit approach', *Computers in Fluids*, **7**, 47–67 (1979).
3. R. L. Sani, P. M. Gresho, R. L. Lee and D. F. Griffiths, 'The cause and cure (!) of the spurious pressures generated by certain FEM solutions of the incompressible Navier–Stokes equations: Part 1', *International Journal for Numerical Methods in Fluids*, **1**(1), 17–43 (1981).
4. R. A. Walters and G. F. Carey, 'Analysis of spurious oscillation modes for the Navier–Stokes and shallow water equations', *TICOM Report, No. 81–3*, University of Texas at Austin, Austin, Texas, July 1981.
5. G. W. Platzman, 'Some response characteristics of finite-element tidal models', *Journal of Computational Physics*, **40**(1), 36–63 (1981).
6. W. G. Gray and D. R. Lynch, 'Time-stepping schemes for finite element tidal model computations', *Advances in Water Resources*, **1**, (2), 83–95 (1977).

7. G. F. Carey, 'Some remarks on finite element analysis of viscous flow equations', *Proceedings of the Third International Conference on Finite Elements in Water Resources*, International Society for Computational Methods in Engineering, University of Mississippi, Oxford, May 1980.
8. C. E. Pearson and D. F. Winter, 'On the calculation of tidal currents in homogeneous estuaries', *Journal of Physical Oceanography*, **7**(4), 520–531 (1977).
9. D. R. Lynch and W. G. Gray, 'A wave equation model for finite element tidal computations', *Computers in Fluids*. **7**(3), 207–228 (1979).
10. N. S. Heaps, 'Linearized vertically-integrated equations for residual circulation in coastal seas', *Deutsche Hydrographische Zeitschrift*, **30,** 147–169 (1978).
11. R. A. Walters and R. T. Cheng, 'Accuracy of an estuarine hydrodynamics model using smooth elements', *Water Resources Research*, **16**(1), 187–195 (1980).
12. B. M. Jamart and D. F. Winter, 'Finite element solution of the shallow water wave equations in Fourier space, with application to Knight Inlet, British Columbia', *Proceedings of the Third International Conference on Finite Elements in Flow Problems*, Vol. 2, University of Calgary, July 1980, pp. 103–112.
13. G. F. Pinder and W. G. Gray, *Finite Element Simulation in Surface and Subsurface Hydrology*, Academic Press, New York, 1977.
14. R. A. Walters, 'The frontal method in hydrodynamics simulations', *Computers in Fluids*, **8,** 265–272 (1980).
15. F. D. Malone and J. T. Kuo, 'Semi-implicit finite element methods applied to the shallow water equations', *Journal of Geophysical Research*, **86**(C5), 4029–4040 (1981).
16. D. R. Lynch, 'Comparison of spectral and time-stepping approaches for finite element modeling of tidal circulation', *OCEANS, IEEE No. 81CH165-7*, September 1981, pp. 810–814.
17. C. Le Provost, G. Rougier and A. Poncet, 'Numerical modeling of the harmonic constituents of the tides, with application to the English Channel'. *Journal of Physical Oceanography*, **11,** 1123–1138 (1978).